

## Methods for measuring the infrared spectra of biological cells

**Judith R Mourant, Rowena R Gibson, Tamara M Johnson,  
Susan Carpenter, Kurt W Short, Yujiro R Yamada  
and James P Freyer**

Bioscience Division, MS E535, Los Alamos National Laboratory, Los Alamos, NM 87545, USA

Received 23 July 2002, in final form 27 November 2002

Published 8 January 2003

Online at [stacks.iop.org/PMB/48/243](http://stacks.iop.org/PMB/48/243)

### Abstract

Infrared (IR) spectroscopy of biological cells is a growing area of research, with many papers focusing on differences between the spectra of cancerous and noncancerous cells. Much of this research has been performed using a monolayer of dehydrated cells. We posit that the use of monolayers can introduce artefacts that lead to an apparent but inaccurate measurement of differences between cancerous and noncancerous cells. Additionally, the use of dried cells complicates the extraction of biochemical information from the IR spectra. We demonstrate that using suspensions of viable cells in aqueous suspension reduces measurement artefacts and facilitates determining the concentration of the major biochemical components via a linear least-squares fit of the component spectra to the spectrum of the cells.

### 1. Introduction

Many of the reported measurements of infrared (IR) spectra have been performed on dried cells (Boydston-White *et al* 1999, Ramesh *et al* 2001, Cohenford and Rigas 1998). The IR spectra of dried cells may differ from the IR spectra of cells in their natural aqueous state since the spectra of many of the known biochemical components of cells change with hydration level. The IR spectra of proteins have been shown to change dramatically after dehydration (Dong *et al* 1996, Pevsner and Diem 2001a, Prestrelski *et al* 1993, Jackson and Mantsch 1995, van de Weert *et al* 2001). Absorption bands can shift and change in amplitude as a function of hydration. The spectra of nucleic acids also depend on hydration status. As RNA and DNA are hydrated, the phosphate absorption bands narrow (Pevsner and Diem 2001b) and the conformation of DNA can be altered (Kim *et al* 1997).

In addition to spectral artefacts caused by dehydration of the sample, another potential source of spectral distortions is inhomogeneity of the sample. As presented in the results section, the absorption spectrum of a material can differ depending on whether the sample is homogeneous or heterogeneous. Three potential causes of sample inhomogeneity are

described below: a nonuniform distribution of cells on a substrate; differences in the height of different portions of cells on a substrate; and inhomogeneity of biochemical components within cells.

Many IR absorbance measurements of cells have been performed with 50–100  $\mu\text{m}$  diameter beams on monolayers which may not be uniform. The manner in which cells attach in monolayer culture depends on the individual type of cell and the cells may not uniformly cover the substrate. In particular, cancerous cells may have unusual attachment patterns. The difference in growth between non-tumourigenic M1 fibroblasts and their tumourigenic T24Ha-*ras*-(co)-transfected counterpart, MR1 fibroblast cells, provides an example of the diversity of how cells grow. When M1 cells grow to confluence, they completely cover the surface. MR1 cells, however, will not completely cover the surface, there are always void areas. The cells will begin to detach and grow on top of each other before completely covering the surface. A second example of the differences in morphology upon oncogenic transformation is the difference between MDCK epithelial cells and their *ras*-transformed counterpart, R5 cells (Hoh and Schoenberger 1994). MDCK cells form homogeneous monolayers, while R5 cells spread out and often extend processes.

Surface height variations are more pronounced for R5 cells than for MDCK cells and are another source of inhomogeneity in cell monolayers. When cells grow on a slide, they typically spread out and form a thin layer only a few  $\mu\text{m}$  thick (Domke *et al* 2000). The nucleus, however, does not spread out as thinly as the cytoplasm. For example, the periphery of R5 cells may be only 200 nm thick while the nuclei are sometimes more than 5  $\mu\text{m}$  thick (Hoh and Schoenberger 1994). Consequently, DNA, which is found primarily in the nucleus, is only found over a fraction of the surface.

Another possible cause of sample inhomogeneity is a nonuniform distortion of biochemicals within the nucleus or the cytoplasm. Because most of this heterogeneity is significantly below the diffraction limit of IR light, these effects are not expected to be significant. Nonetheless, relatively large, dense patches of chromatin could, in principle, cause an artefact in the absorption measurement by blocking light from passing in some locations, as suggested by Diem and co-workers (Boydston-White *et al* 1999). The DNA absorption would then appear artificially low because in some places there would be no DNA while in a few locations the light would be completely blocked. The organization and packing of the DNA depends strongly on the cell cycle (El-Alfy 1998). At the beginning of the synthesis phase of the cell cycle (S-phase), heterochromatin (a condensed, transcriptionally inactive fibrous complex of DNA and histone proteins) lines the nuclear envelope and the nucleoli are evident. As synthesis progresses, threads and aggregates of DNA become apparent and the nucleoli become more prominent. Aggregates of DNA are present during G2. At mitosis, the DNA condenses into chromosomes and the cell divides. In the G1 phase after cell division, the DNA decondenses. Therefore, it is only during part of mitosis that condensed chromosomes form micron-sized structures of dense DNA. Since mitosis is a small fraction of the cell cycle, for example, 15 min out of 12–14 h, only about 1–2% of the cells may be in a state in which the DNA is so dense that wavelengths of light absorbed by DNA cannot penetrate through a cell.

One reason for making IR spectroscopic measurements rather than using a different spectroscopic technique that might also be able to differentiate cancerous and noncancerous cells is that IR spectroscopy can provide biochemical information. In principle, IR spectroscopy can provide quantitative information on the biochemical composition of the cells, because different compounds have distinct spectra. There are four primary biochemical constituents of cells: DNA, RNA, protein and the phospholipids. Sugars such as glycogen can also be a significant constituent. An open question is how well a linear combination

of these components measured *in vitro* can reproduce the IR spectrum of cells. If it is reproduced well, then IR spectroscopy has good potential to noninvasively provide biochemical information.

## 2. Materials and methods

### 2.1. Cell lines

The non-tumourigenic rat fibroblast cell line, M1, and its highly tumourigenic counterpart, MR1, were derived by first *myc*-transfecting Fisher 344 rat embryo fibroblasts to obtain the M1 cell line and then by transfection with the point-mutated T24Ha-*ras*-oncogene to obtain the MR1 cell line (Kunz-Schughart *et al* 1995). AT3.1 cells are androgen-independent malignant rat prostate carcinoma cells kindly supplied by Dr Rinker-Schaeffer of the University of Chicago (Tennant *et al* 2000).

### 2.2. Preparation of viable cell suspensions

Cells were cultured as monolayers in standard tissue culture flasks using Dulbecco's modified eagle's medium (INVITROGEN) containing 4.5 g l<sup>-1</sup> D-glucose 5% (v/v) foetal calf serum (HYCLONE), 100 IU ml<sup>-1</sup> penicillin and 100 µg ml<sup>-1</sup> streptomycin, referred to as complete medium hereafter. Cell suspensions were obtained from monolayer cultures by treatment for 10 min with 0.25% trypsin in Dulbecco's phosphate buffered saline (PBS, INVITROGEN) with 1 mM EDTA at pH 7.4. The cell suspensions were prepared by the addition of cold complete medium, passage twice through an 18 gauge needle, then centrifuged to form a pellet and resuspended in PBS at 1 × 10<sup>8</sup> to 3 × 10<sup>8</sup> cells ml<sup>-1</sup>. To verify the concentration and determine cell volumes, an aliquot of each cell suspension was counted using an electronic particle counter interfaced to a pulse-height analyser (Coulter Electronics). During the counting, a cell-volume distribution was acquired and used to estimate cell diameters.

### 2.3. Transmission IR measurement

The IR spectra were obtained in transmission mode. The sample cell consisted of two rectangular barium fluoride windows held in apposition with an oval-shaped 50 µm thick ring of teflon between them. The top window had two holes, one at the top and one at the bottom, for loading the sample. A rubber gasket was placed over the top window to seal the holes and prevent the sample from leaking out. The fibroblast cells were loaded into the 50 µm thick sample space between two BaF<sub>2</sub> windows by using a syringe through one of the holes in the top window to push the cell suspension into the sample space while a needle in the other hole allowed air to escape during the loading process. The IR beam spot was ~1 cm in diameter and the spectra were obtained at 2 cm<sup>-1</sup> resolution with 200 scans taken per spectrum. Collection time for a single spectrum on our Fourier transform IR spectrometer (FTIR, Mattson Cygnus-100) was 7 min. The cells were not on ice during the measurement, however we have found that this amount of time at room temperature does not affect the viability of the cells (Omberg *et al* 2002). A typical measurement protocol consisted of taking two spectra of PBS, two spectra of cells, two spectra of PBS, two spectra of cells and two spectra of PBS. The absorption of the cells is calculated as shown in equation (1) where  $I_{\text{cells,ave}}$  is the average of the intensity measured when cells were in the sample chamber and  $I_{\text{PBS,ave}}$  is the average of the spectra of PBS. At very low signal levels, the calculated absorption will be slightly distorted. For our instrument and measurement conditions, we found that there was significant signal between 940 and 1565 cm<sup>-1</sup>, and between 2800 and 2940 cm<sup>-1</sup> such that

there was no distortion. The only baseline correction performed was adding or subtracting a constant.

$$\text{Absorbance} = -\log\left(\frac{I_{\text{cells\_ave}}}{I_{\text{PBS\_ave}}}\right). \quad (1)$$

For the measurement of dried cells, a thin layer of hydrated cells was placed on a BaF<sub>2</sub> window. The window was then placed in a refrigerator and the cells dried out over a period of several hours. The sample cell was then assembled (the dried cells were inside the ring-shaped spacer) and IR absorption measurements were performed. The number of dried cells in the light path of the FTIR is expected to be much higher than for the corresponding case of cells in aqueous medium. The reference for these measurements is an empty cell.

#### 2.4. Measurement of biochemical components

The expected major biochemical components of cells were measured in aqueous media. Type I, 'highly-polymerized' calf thymus DNA (Sigma, D-1501), was dissolved in TE buffer (pH 8.02, 10 mM Tris, 1 mM EDTA) at a concentration of 10 mg ml<sup>-1</sup>. Similarly, calf liver RNA (Sigma, D-1501) was dissolved in TE buffer at a concentration of 10 mg ml<sup>-1</sup>. Glycogen (Sigma, G-0885) was measured at 10 mg ml<sup>-1</sup> in pH 7 phosphate buffer. Liver lipid extract in chloroform was obtained from Avanti (cat. no 181108). Chloroform was removed by blowing argon over the sample in a fume hood. The sample was then dissolved in a buffer consisting of 0.01 M, pH 7.3 Tris, 0.1 M NaCl and 0.02 M sodium azide. The total concentration of lipids was 25 mg ml<sup>-1</sup>.

In order to obtain a spectrum of protein that represents the protein components of the cells, we measured protein isolated from the cells. Cells on which IR absorbance measurements were completed were centrifuged to a pellet, frozen and stored until the protein was needed. For the initial extraction, the cells were resuspended with tissue protein extraction reagent (TPER) (Pierce product no 78510) and protease inhibitors. The masses per ml of TPER were 0.05 g of cells, 1 μg of aprotinin, 10 μg of phenylmethylsulfonylfluoride and 1 μg of leupeptin. One millimolar dithiothreitol (DTT) was also used. The suspension was sonicated for three 10 s periods and subsequently centrifuged for 10 min at 4 °C. The supernatant was then run on an equilibrated size exclusion column (Biogel A 0.5) to purify the protein. The column was prepared by washing three times with 150 mM NaCl and the protein was run with 150 mM NaCl and 1 mM DTT at pH 7.5. Three fractions were collected and concentrated by ultrafiltration using a 200 ml stirred cell (Amicon, PM-30 10 000 MW filter), and the concentration of protein in each fraction determined by Bradford assay. The first fraction contained a large amount of cell debris. The second fraction contained a large amount of protein (~7 mg ml<sup>-1</sup>) without cell debris. The molecular weight of the proteins in this fraction ranged from 10 to 100 kD. The third fraction did not contain sufficient protein to perform IR measurements.

In order to obtain the absorption of each biochemical component, the component dissolved in buffer and the buffer alone were measured. The absorbance was then calculated via an equation analogous to equation (1).

#### 2.5. Fitting the measured IR spectra of cells to a linear sum of the biochemical components

The measured IR spectra were fit to a linear sum of the measured IR spectra (lipid, RNA, DNA, protein, glycogen and PBS) and baseline spectra such that the square of the difference between the absorbance measurement and the fit was minimized. The baseline spectra were a constant and a linear term for the low frequency part of the spectrum, and a constant and

a linear term for the high frequency part of the spectrum. The minimization was performed using a linear least-squares method which utilized singular value decomposition in order to avoid singularities which can occur when several combinations of the basis functions fit the data almost equally well (Press *et al* 1997).

### 2.6. Computation of the effects of sample heterogeneity on the FTIR spectra of cells

For a given uniform concentration of a biochemical compound, the measured absorption on a standard transmission FTIR will be

$$A = \varepsilon(\lambda)CL \quad (2)$$

where  $\varepsilon(\lambda)$  is the molar extinction coefficient,  $C$  is the concentration and  $L$  is the pathlength. When the concentration is uniformly cut in half, the absorption becomes  $\varepsilon(\lambda)CL/2$ . If instead of cutting the concentration in half, the coverage of the surface is reduced to 50%, the absorption becomes

$$A = -\log\left(\frac{(10^{-\varepsilon CL} + 1)}{2}\right). \quad (3)$$

Equations (2) and (3) can be used to estimate the spectral changes likely to occur when cells are not uniformly distributed on a substrate.

In the case of a suspension of cells in a thin transmission FTIR cell, the calculation of sample heterogeneity is more difficult. For our calculations, we examined  $20 \mu\text{m} \times 20 \mu\text{m} \times 50 \mu\text{m}$  volumes, i.e., volumes that had a cross-sectional area to the IR beam of  $20 \mu\text{m} \times 20 \mu\text{m}$ . The volume of cells in each voxel was calculated using Monte Carlo methods. The location of each cell in the sample was chosen by sampling three uniform distributions, each representing one dimension. If the cell physically overlapped with another cell, new coordinates were chosen. After all the cells were placed, the volume fraction of cells in each voxel was computed. If only part of a cell was in the voxel, then only the volume fraction of the cell in the voxel was counted. The cells were assumed to have a diameter of  $14 \mu\text{m}$  based on measured volume distributions of M1 and MR1 cells.

### 2.7. Measurement of Raman spectra

Excitation was provided by a 785 nm diode laser (Invictus NIR Laser, Kaiser Optical Systems). Light was delivered and collected from the sample using fibre optics (Mark II filtered probe head, Kaiser Optical Systems) onto which a 16 mm diameter  $f/0.7$  aspheric condenser lens was attached. Light collection was performed through the same lens. The collected light was dispersed by a spectrograph with a holographic grating (Holospec F1.8i, Kaiser Optical Systems) with a  $100 \mu\text{m}$  slit and collected by a liquid-nitrogen-cooled, deep-depletion, back-illuminated CCD camera (Spec-10:100BR, Princeton Instruments). The aqueous sample was placed in an NMR tube for measurement. The dried samples were dried in a refrigerator on a  $\text{MgF}_2$  window and subsequently measured.

For analysis, the fluorescence from the optics, and, in the case of the hydrated cells, the NMR tube and the phosphate buffer were subtracted from the spectra. Residual background fluorescence from the cells was then subtracted by picking regions of the spectrum which did not show obvious Raman peaks and fitting a cubic spline through these regions.

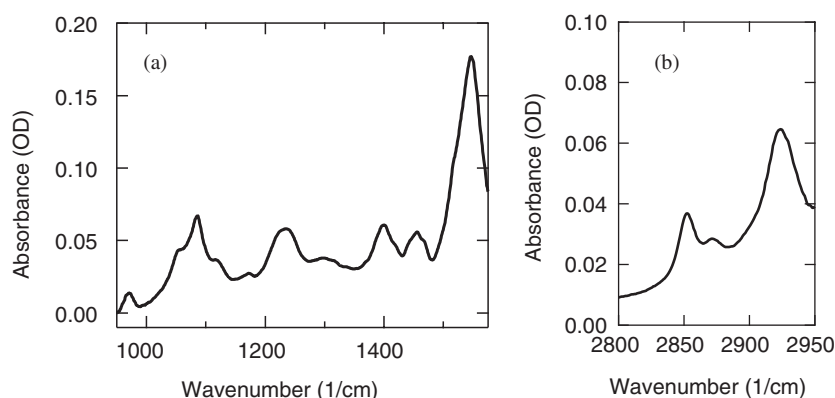


**Figure 1.** FTIR absorption spectra of MR1 fibroblast cells in aqueous media. Spectra are shown from 950 to 1575  $\text{cm}^{-1}$  (a) and from 2800 to 2950  $\text{cm}^{-1}$  (b). The cell concentration was about  $3 \times 10^8$  cells  $\text{ml}^{-1}$  and the measurement pathlength was 50  $\mu\text{m}$ . No baseline correction has been performed.

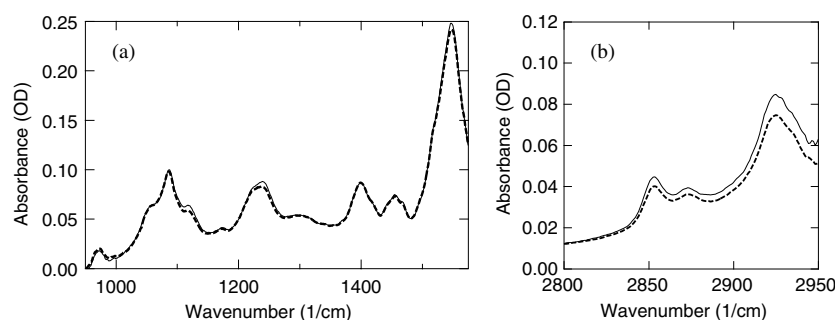


**Figure 2.** IR absorbance spectra of epithelial and fibroblast cells. Solid line: MR1 fibroblast cells. Thick dashed line: AT3.1 epithelial cells. The spectra have been scaled so that the absorbance at the 1400  $\text{cm}^{-1}$  peak is the same.

### 3. Results

#### 3.1. FTIR measurements and analysis of FTIR measurements of hydrated cells

The absorption spectra of MR1 fibroblast cells in aqueous solution are shown in figure 1. The spectra generally resemble the spectra published for monolayers of cells (Boydston-White *et al* 1999, Ramesh *et al* 2001) with the exception that amide I is not shown. Absorption between 1575 and 1710  $\text{cm}^{-1}$  cannot be measured because strong water absorption prevents light from reaching the detector. These results demonstrate that spectra with good signal to noise can be obtained from mammalian cells in an aqueous environment.

In addition to measuring the absorption of fibroblast cells in aqueous suspension, we have also measured the absorption spectra of epithelial cells. Figure 2 compares the spectra of AT3.1 epithelial cells to the spectra of MR1 fibroblast cells. Despite the large differences in biological function, the spectra are very similar. The differences in the 2800–2950  $\text{cm}^{-1}$  region are primarily due to baseline artefacts as this region is highly susceptible to such artefacts due to the rapidly changing water absorption as a function of wavelength in this region.

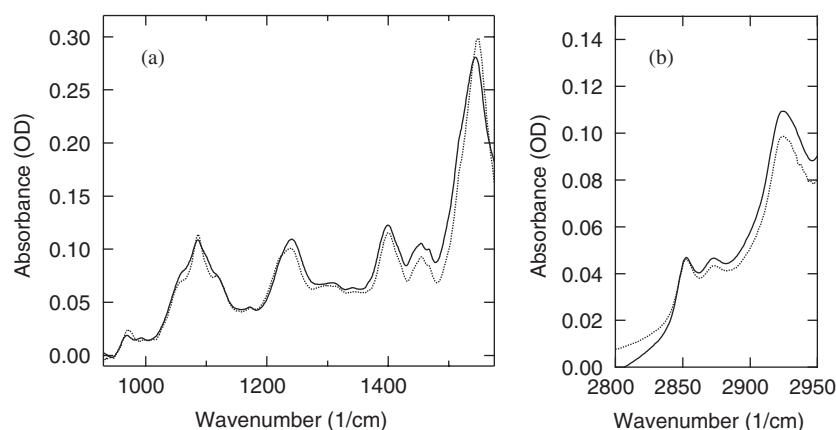


**Figure 3.** Comparison of the IR spectra of M1 cells in aqueous media compared to the spectra of the same cells after they have been dried. Solid line: dried cells. Dashed line: cells in aqueous media. The spectra of the dried cells was divided by a factor of 4.

### 3.2. Comparison of absorbance measurements of hydrated and dried fibroblast cells

FTIR spectra of M1 fibroblast cells harvested in the exponential phase of growth were measured at a concentration of  $1.9 \times 10^8$  cells  $\text{ml}^{-1}$ . The cells were then allowed to dry in the refrigerator and re-measured. Figure 3 shows a comparison of the spectra of dried cells versus the spectra of viable cells in aqueous media. There are several noticeable differences. The phosphate absorption bands of RNA and DNA between  $1050$  and  $1150$   $\text{cm}^{-1}$  are not as well defined for the dried cells. The shape and position of the absorption band near  $1225$   $\text{cm}^{-1}$  changed when the cells were dried. Amide II has a reduced intensity relative to the other absorption bands and it is shifted to shorter wavenumbers for the spectra of dried cells. This change in position of amide II indicates that the secondary structure of proteins is altered when the cells are dried. Very similar results to those obtained for M1 cells were also obtained for MR1 fibroblast cells harvested in the plateau phase of growth.

The change in biochemical spectra was verified using Raman scattering. Figure 4(a) shows the Raman spectra of MR1 cells both in aqueous solution and dried. There are striking differences which can be attributed to changes in both the nucleic acids and the proteins. First, there are significant changes in the amide I region of the spectra as shown in more detail in figure 4(b). The shape of the amide I peak changes. In the spectrum of cells in solution, the peak at  $1671$   $\text{cm}^{-1}$  is due to  $\beta$ -sheet structures, the peak at  $1648$   $\text{cm}^{-1}$  due to  $\alpha$ -helix structures and the peak centred near  $1660$   $\text{cm}^{-1}$  likely represents a mixture of  $\alpha$ -helix,  $\beta$ -turn and undefined structures (Spiro and Garber 1977, Williams and Dunker 1981). These peaks are clearly above the noise as evidenced by the difference in intensity at  $1667.8$  and  $1671.4$   $\text{cm}^{-1}$ , being  $0.038 \pm 0.017$  for the 10 spectra of hydrated spectra of cells. Drying the cells results in a more symmetric amide I peak with no shoulders, centred near  $1656$   $\text{cm}^{-1}$ . This suggests either a change in protein secondary structure and/or a change in the hydrogen bonding in the cell proteins due to loss of water. Changes in amide I position and shape have been observed before in studies where dried and hydrated proteins and peptides are compared (Yu *et al* 1972, Hruby *et al* 1978). The interpretation of these earlier results was difficult and in some instances it was argued that changes in the water absorption underlying the amide I absorption were responsible for the change. The changes described in this paper between

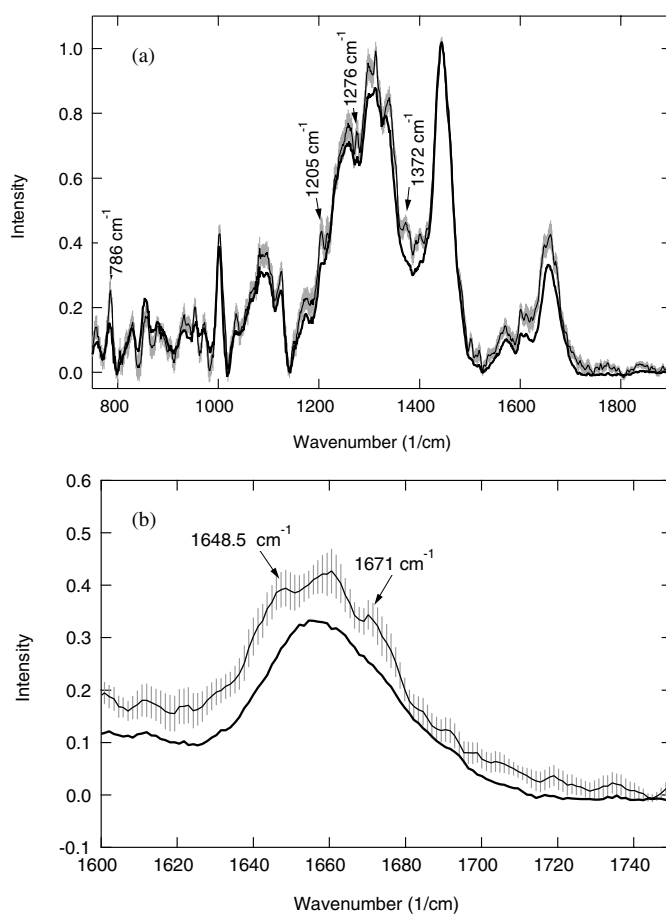


**Figure 4.** (a) Raman spectra of hydrated and dried MR1 cells in the plateau phase of growth. The thin black line is the average of 10 spectra of aqueous cells. The standard deviations are shown in grey. The thick black line is a measurement of the dried cells. The spectra were normalized to have the same integrated intensity from 1442 to 1449  $\text{cm}^{-1}$ . (b) Expanded view of the amide I region in (a).

the hydrated and dried cells cannot be duplicated by subtracting from the hydrated spectrum differing amounts of the water peak which occurs near the same position as the amide I peak.

Some other examples of Raman spectral changes upon drying the cells are intensity decreases of peaks at 786 and 1276  $\text{cm}^{-1}$ . Nucleic acids have a very strong absorption band at 786  $\text{cm}^{-1}$  (Small and Peticolas 1971). Neither proteins nor lipids have a strong absorption at this frequency. Therefore, the decrease in intensity at 786  $\text{cm}^{-1}$  indicates a change in the nucleic acid conformation. The peak at 1276  $\text{cm}^{-1}$  can be assigned to amide III  $\alpha$ -helix structures (Spiro and Garber 1977, Williams and Dunker 1981, Parker 1983), indicating, again, changes in protein structure and/or environment.

### 3.3. Distortions of the spectra due to a nonuniform sample

As described in the introduction, some types of cells will not form a uniform monolayer of cells in culture. In order to understand how the FTIR spectra of a uniform layer of cells differs

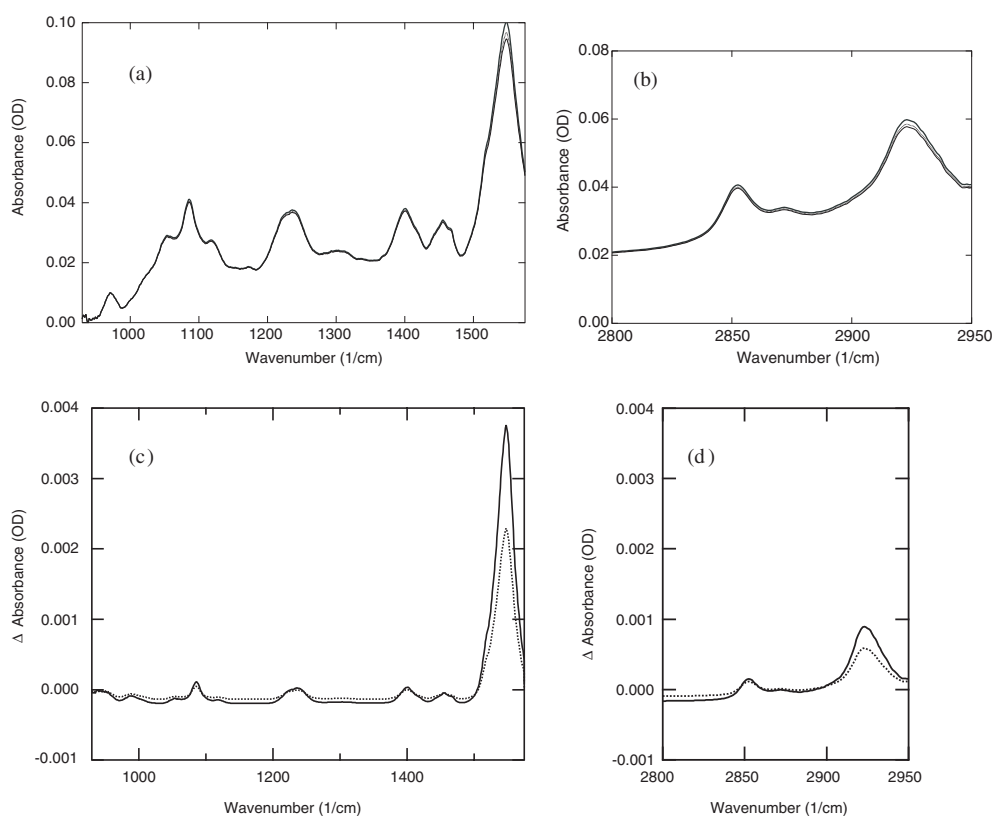


**Figure 5.** (a) and (b) The effect of inhomogeneity of biochemical components on FTIR absorption measurements. The transmission spectrum of a sample with homogeneous biochemical components was assumed to be given by the thick solid line. The absorption spectrum in the case that the sample only covered half the area interrogated by the IR beam was then calculated as described in the text and is shown as the thin solid line. The spectrum is distorted at the amide II absorption. The distortion of the IR spectrum due to the inhomogeneity of an aqueous sample in our FTIR sample cell is shown as the thin dashed line. Again there is some distortion at the amide II absorption. (c) and (d) Difference in the apparent absorption when the sample is homogeneous or inhomogeneous. Solid line—when the sample only covers half the surface area. Dashed line—an aqueous sample with a concentration of  $10^8$  cells  $\text{ml}^{-1}$ .

from a nonuniform layer of the same cells, model calculations were performed. A theoretical spectrum of a uniform layer of cells is given by the thick solid black curve in figure 5(a). The measured absorption in the case that 50% of the slide is covered by void areas can be calculated using equation (3) and the original spectrum. We assume that the volume of cells stays constant. Distortion of the spectrum is given by the thin solid line in figures 5(a) and (b). The difference between the theoretical spectrum and the spectrum of 50% coverage is shown in figures 5(c) and (d) by the solid line. The relative intensity of amide II is reduced when coverage of the surface is incomplete. Consequently, peak ratios change, the ratio of the peak of amide II at  $1549 \text{ cm}^{-1}$  to the phosphate peak at  $1086 \text{ cm}^{-1}$  changes from 2.47 to 2.38.

When cells are measured in aqueous suspension, as for our transmission measurements shown in figure 1, the cell suspension is still not uniform. In order to model this situation, the sample cell volume was divided into volume elements of  $20 \mu\text{m} \times 20 \mu\text{m} \times 50 \mu\text{m}$ . The  $50 \mu\text{m}$  dimension is along the direction of transmission through the sample cell. The

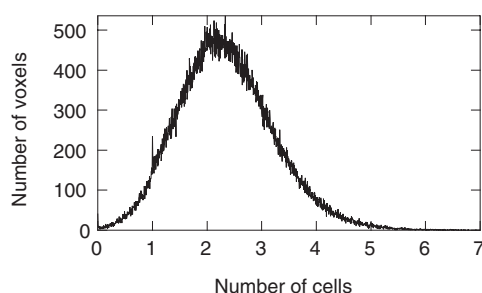


**Figure 6.** Distribution of the number cells per voxel.

number of cells in each of these voxels was then calculated assuming a cell concentration of  $10^8$  cells  $\text{ml}^{-1}$ . As shown in figure 6, the number of cells per voxel varies from 0 to  $\sim 5$  with the majority of voxels containing two to three cells. Based on this distribution, the distortion of the absorbance spectrum was calculated and is shown in figures 5(a) and (b) by the thin dashed line. The difference between the theoretical spectrum and the spectrum of aqueous cells is shown in figures 5(c) and (d) by the dashed line. The error for the aqueous measurements is less than for the 50% monolayer measurements.

#### 3.4. Distortions of the measurements due to displacement of PBS

The absorbance of the cells is calculated according to equation (1). This equation is not strictly correct if the solid components of the cells displace some of the PBS. The absorbance described in equation (1) is given by equation (4), where  $A_{\text{PBS}}$  is the absorbance spectra of the PBS,  $A_{\text{cells}}$  is the true absorbance spectra of the cells and  $f_{\text{PBS}}$  is the fractional change in the volume of PBS, i.e., if the cells displaced 1% of the volume of PBS, then  $f_{\text{PBS}} = 0.01$ .

$$A = -f_{\text{PBS}}A_{\text{PBS}} + A_{\text{cells}}. \quad (4)$$

Based on our measurements of the absorption of PBS, it only takes a very small displacement of PBS (1–2%) to cause a distortion in the measured spectrum. Using specific volumes for the cell constituents and estimates of their concentration, we found that at our cell concentration about 1.6% of the PBS volume is displaced by solids.

#### 3.5. Linear combination of the primary biochemical components

In order to understand the biochemical composition of the cells, we measured spectra of the expected biochemical components of the biological cells. IR spectra of lipid, RNA, DNA and protein are shown in figures 7(a) and (b). RNA and DNA do not absorb between 2800 and 2950  $\text{cm}^{-1}$ , therefore they are not shown in figure 7(b). The protein was isolated from MR1 cells harvested in the plateau phase of growth. In addition to these spectra, a spectrum of glycogen which absorbs between 1000 and 1200  $\text{cm}^{-1}$  was also used but was found to play a very minor role and PBS was also used to fit the measured cell spectrum for the reasons discussed above. Both the low frequency (930–1575  $\text{cm}^{-1}$ ) and the high frequency region (2800–2950  $\text{cm}^{-1}$ ) were fit simultaneously and the result of a linear least squares fit of the component spectra to the measured absorption spectra of aqueous MR1 cells harvested in the exponential phase of growth is shown in figure 8(a). The fit reproduces the major features of the MR1 cells absorption spectra. There are, however, a few discrepancies, as can be seen by examining the residuals plotted in figure 8(b). For example, the amide II band is shifted. There are also differences between the fit and the measured data between 1100 and 1200  $\text{cm}^{-1}$ .

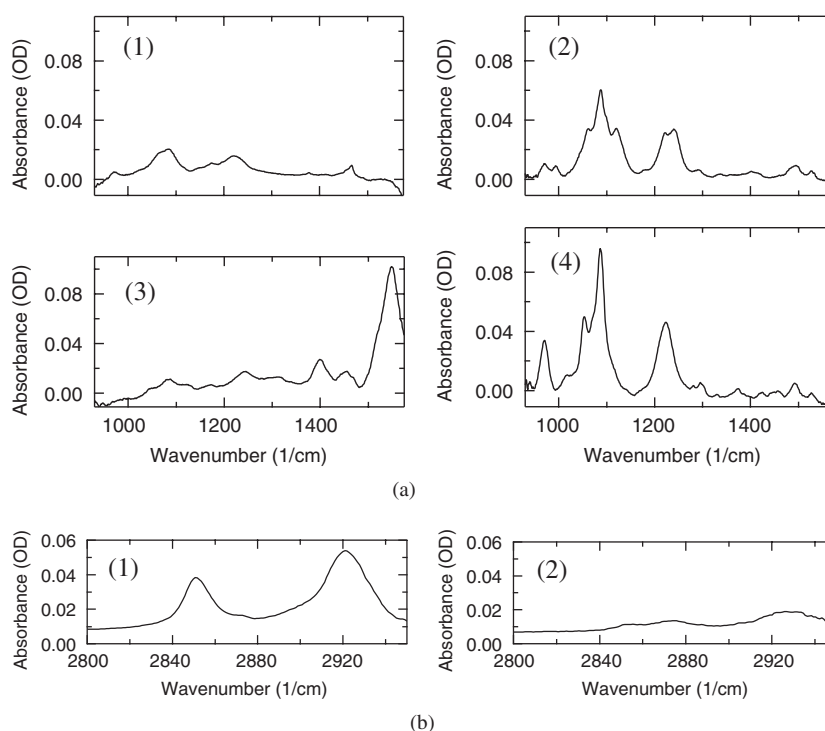


**Figure 7.** (a) Spectra of the major biochemical components of cells absorbing between  $930$  and  $1585\text{ cm}^{-1}$ : (1) lipid; (2) RNA; (3) protein and (4) DNA. (b) Spectra of the major biochemical components of cells absorbing between  $2800$  and  $2950\text{ cm}^{-1}$ : (1) lipid; (2) protein.

#### 4. Discussion

Figure 1 demonstrates that high quality IR absorption spectra can be obtained of mammalian cells in aqueous suspension. Figure 2 demonstrates that spectra of fibroblast and epithelial cells are very similar. Given the extremely different function of these two types of eukaryotic cells, this result is somewhat surprising. This result indicates that the gross biochemical composition of eukaryotic cells may not vary greatly. Therefore, great care must be taken in order to accurately measure absorbances so that any small differences that may exist can be found.

Drying of cells introduces artefacts as compared to the spectra of cells in aqueous suspension. Both the Raman and the IR spectra indicate that there are changes in the nucleic acids as well as in the conformation of the proteins. The argument might be made that measuring dried cells is acceptable as long as the cells are always dried. However, this may not be the case. The relative humidity of the laboratory where the cells are measured may affect the measurements such that absorbance spectra from different laboratories or at different times cannot be compared. In principle, humidity can be controlled with an appropriate sample cell, although this may increase the cost and complexity of the experiment. Even if humidity is accurately controlled, the dehydration of a sample can complicate the biochemical analysis of a sample. In order to biochemically analyse a complex sample, such as a biological cell, spectra are needed of isolated components in an environment that mimics the internal environment of cells. Therefore, isolated components (i.e., RNA, DNA, phospholipid and protein) must be measured at the same level of hydration as is found in the dehydrated

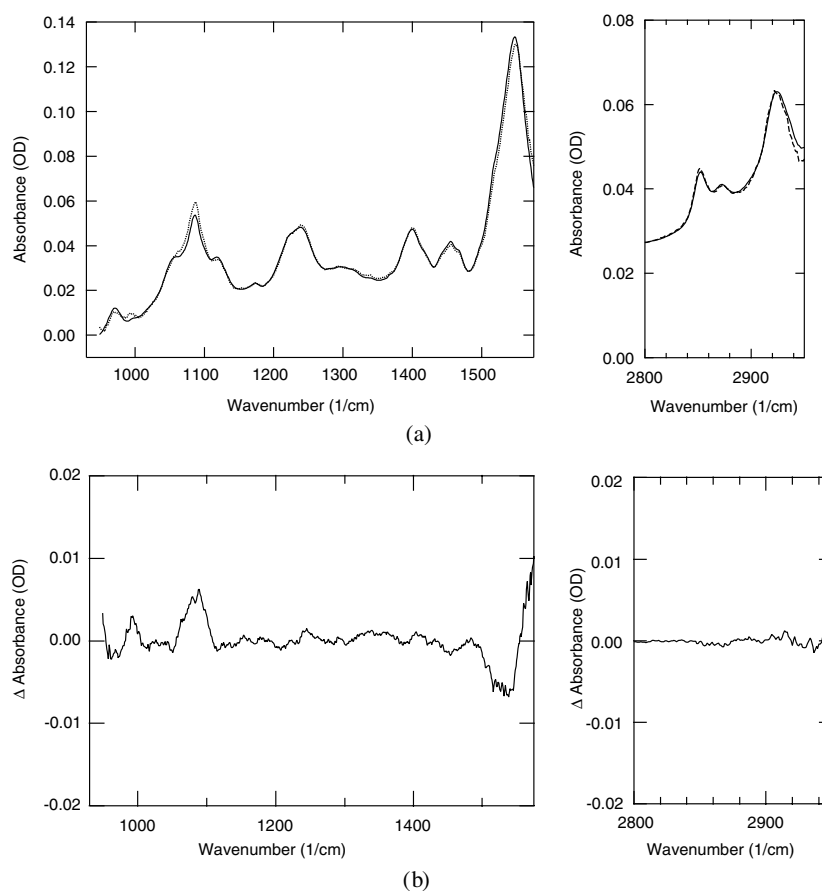


**Figure 8.** (a) Linear least-squares fit of the spectra of MRI cells to the major biochemical components of the cell. The data are shown as a solid line. The fit is the dashed line. (b) Residuals from a linear least squares fit of the spectra of MRI cells to the major biochemical components of the cell.

samples. These requirements complicate the determination of biochemical composition from dehydrated samples. A final important point is that the long-term goal of this work is to develop tools for optical diagnosis of cancer in humans. This endeavour will obviously involve measuring vibrational spectra under hydrated conditions, so differences observed between malignant and normal cells using dried samples may well have little relevance to cancer diagnosis.

Another source of spectral distortion can be nonuniformity of the sample. The results of two calculations were presented, which illustrate the magnitude of the problem. Samples that are inhomogeneous will have an apparent decrease in absorbance of the strongest absorption bands. The distortion for amide I would be even greater than the distortion shown for amide II since amide I absorption is greater than that of amide II. The distortions due to localization of DNA, RNA and phospholipid are not expected to be nearly as significant as the distortions of the spectra due to localization and heterogeneity of the distribution of the protein within the sample because the absorption of protein varies much more strongly across the spectrum.

Aside from differences in the homogeneity of the sample, there are other potential differences in samples of cancerous and noncancerous cells that can lead to ascribing a

difference in the IR spectra of the samples to an intrinsic difference between the cancerous and noncancerous cells when there is no such difference. Several groups have reported that the IR spectra of cells depend on the cell cycle (Boydston-White *et al* 1999, Holman *et al* 2000). In culture, different types of cells grow differently. Consequently, one cell type grown for four days may still be dividing while another cell type kept under the same conditions could be growth arrested. Dividing cells will have a different cell cycle distribution and consequently a different IR spectrum than the cells that are growth arrested. Therefore, even when there is no intrinsic biochemical difference in the cells, a difference in how the cells grow may appear as a difference in the FTIR spectra of the cells.

One possibility for decreasing and possibly eliminating errors due to the nonuniformity of the sample would be to measure a multicellular membrane (Wilson and Hics 1999, Cowan *et al* 1996). A multicellular membrane is a three-dimensional cell model system consisting of multiple layers of cells growing on top of a porous membrane. The cells are packed tightly on top of each other instead of being round, as they are in suspension. For a thickness of ten or more cell layers, the biochemical composition across the cells should be nearly uniform. This thickness should not cause an absorbance that is great enough to block light from reaching the detector. Based on our measurements of fibroblast cells in figure 1 and the results in figure 6, the absorption at amide II will be less than 0.75 OD. Multicellular membranes are very similar to the structure of tissues *in vivo* in terms of cell growth, morphology, and the ratio of intra- to extracellular space.

Figure 8 demonstrates that spectra of mammalian cells can very nearly be described by a linear superposition of the spectra of the biochemical components that constitute the cell. Future work is needed to determine the cause of the differences between the fit and the measured data. One potential concern is that the proteins which are isolated from the cells may not accurately represent the variety of proteins found in the cells. We have found that there is some variation in our absorbance results for protein extractions from different types of cells. Other possibilities for the discrepancies between the fits and the data are that not all the important biological components were included or that the spectra of the biochemical components are different when measured in extractions than in their natural environment. The last possibility is illustrated by our finding that the spectra of DNA broken up into crude oligonucleotides (Sigma, D3159) are quite different from the spectra of mostly double-stranded DNA.

Figure 7 illustrates that the absorption bands of the biochemical components of the cells frequently overlap. Therefore, using peak ratios as measurements of the ratio of biochemical components may be misleading. For example, the ratio of absorbance at  $1121\text{ cm}^{-1}$  to absorbance at  $1020\text{ cm}^{-1}$  has been used as an index for cellular RNA/DNA (Ramesh *et al* 2001). However, phospholipids also absorb at  $1020\text{ cm}^{-1}$ . Therefore the ratio may give erroneous results. From a fit such as the one in figure 8, the concentration of biochemical components can be determined. The results of the fit in figure 8 are that a cell suspension of  $10^8$  MR1 cells per ml in the exponential phase of growth has concentrations of lipid, protein, RNA, DNA and glycogen of  $3.4\text{ mg ml}^{-1}$ ,  $10.3\text{ mg ml}^{-1}$ ,  $4.03\text{ mg ml}^{-1}$ ,  $0.62\text{ mg ml}^{-1}$  and  $0.4\text{ mg ml}^{-1}$ , respectively, and that the volume of PBS displaced by the cells is about 1.2% of the volume of a pure PBS sample. The displacement of PBS determined from the fit can be compared with a calculation of the volumes of the solid components which can be determined by multiplying the concentration of each component by its specific volume. Using estimates of the specific volumes from the literature (Hianik *et al* 1998, Sophianopoulos *et al* 1962, Durchschlag and Zipper 1997), we find that 1.6% of the sample is taken up by solids. Fitting a linear combination of basis spectra to the spectra of cells is much more accurate than using peak ratios since overlapping absorbances are accounted for. With the exception of amide II,

none of the absorption bands is due to a single biochemical component. Therefore, simple peak ratios cannot be used to determine the ratio of biochemical constituents. The accuracy of using a linear least-squares fit to determine the concentration of biochemical components should be tested by comparison with other methods of measuring the concentration of biochemical components.

## 5. Conclusions

There are significant differences between the vibrational spectra of hydrated and dried mammalian cells. In addition to drying, other aspects of sample preparation can alter the measured spectrum. Samples that are inhomogeneous will have an apparent decrease in absorbance of the strongest absorption bands. Furthermore, the IR spectra are expected to depend on whether the cells are in the plateau or exponential phase of growth when they are measured. Spectral artefacts due to drying and sample inhomogeneity can be completely or partially alleviated by measuring aqueous samples. In particular, 'multicellular membranes' could provide an excellent measurement system. Accurate measurements of vibrational spectra may provide a method for assaying cell biochemistry without the need to fix or stain the cells. The IR spectrum of a cell can be closely reproduced with a linear combination of DNA, RNA, phospholipid, glycogen and protein spectra.

## Acknowledgment

Lynne Dominique measured the spectra of RNA and DNA used in the components fits in figure 8.

## References

- Boydston-White S, Gopen T, Houser S, Bargonetti J and Diem M 1999 Infrared spectroscopy of human tissue: V. Infrared spectroscopic studies of myeloid leukemia (ML-1) cells at different phases of the cell cycle *Biospectroscopy* **5** 219–27
- Cohenford M A and Rigas B 1998 Cytologically normal cells from neoplastic cervical samples display extensive structural abnormalities on IR spectroscopy: implications for tumor biology *Proc. Natl. Acad. Sci.* **95** 15327–32
- Cowan D S M, Hickes K O and Wilson W R 1996 Multicellular membranes as an *in vitro* model for extravascular diffusion in tumors *Br. J. Cancer* **74** S26–31
- Domke J, Dannohl S, Parak W J, Muller O, Aicher W K and Radmacher M 2000 Substrate dependent differences in morphology and elasticity of living osteoblasts investigated by atomic force microscopy *Colloids Surf. B: Biointerfaces* **19** 367–79
- Dong A, Matsuura J, Allison S D, Chrisman E, Manning M C and Carpenter J F 1996 Infrared and circular dichroism spectroscopic characterization of structural differences between B-lactoglobulin A and B *Biochemistry* **35** 1450–7
- Durchschlag H and Zipper P 1997 Calculation of partial specific volumes and other volumetric properties of small molecules and polymers *J. Appl. Crystallogr.* **30** 803–7
- El-Alfy M 1998 Introduction to histology of the cell cycle *Microsc. Res. Tech.* **40** 341–3
- Hianik T, Haburcak M, Lohner K, Prenner E, Paltauf F and Hermetter A 1998 Compressibility and density of lipid bilayers composed of polyunsaturated phospholipids and cholesterol *Colloids Surf. A* **139** 189–97
- Hoh J H and Schoenenberger C-A 1994 Surface morphology and mechanical properties of MDCK monolayers by atomic force microscopy *J. Cell Sci.* **107** 1105–14
- Holman H-Y N, Martin M C, Blakely E A, Bjornstad K and McKinney W R 2000 IR spectroscopic characteristics of cell cycle and cell death probed by synchrotron radiation based on Fourier transform IR spectromicroscopy *Biopolymers (Biospectroscopy)* **57** 329–95
- Hruby V J, Deb K K, Fox J and Tu A T 1978 Conformational studies of peptide hormones using laser Raman and circular dichroism spectroscopy *J. Biol. Chem.* **253** 6060–7

- Jackson M and Mantsch H H 1995 The use and misuse of FTIR spectroscopy in the determination of protein structure *Critical Reviews Biochem. Mol. Biol.* **30** 95–120
- Kim J S, Lee S A, Carter B J and Rupprecht A 1997 Stabilization of the B conformation in unoriented films of calf thymus DNA by NaCl: a Raman and IR study *Biopolymers* **41** 233–8
- Kunz-Schughart L A, Simm A and Mueller-Klieser W 1995 Oncogene-associated transformation of early passage rodent fibroblasts is accompanied by large morphologic and metabolic alterations *Oncol. Rep.* **2** 651–61
- Omberg K M, Osborn J C, Zhang S L, Freyer J P, Mourant J R and Schoonover J R 2002 Raman spectroscopy and factor analysis of tumorigenic and non-tumorigenic cells *Appl. Spectrosc.* **56** 313–9
- Parker F S 1983 *Applications of Infrared, Raman, and Resonance Raman Spectroscopy in Biochemistry* (New York: Plenum) p 85
- Pevsner A and Diem M 2001a Infrared spectroscopic studies of major cellular components: Part I. The effect of hydration on the spectra of proteins *Appl. Spectrosc.* **55** 788–93
- Pevsner A and Diem M 2001b Infrared spectroscopic studies of major cellular components: Part II. The effect of hydration on the spectra of nucleic acids *Appl. Spectrosc.* **55** 1502–5
- Press W H, Teukolsky S A, Vetterling W T and Flannery B P 1997 *Numerical Recipes in C* 2nd edn (New York: Cambridge University Press) ch 15
- Prestrelski S J, Tedeschi N, Arakawa T and Carpenter J F 1993 Dehydration-induced conformational transitions in proteins and their inhibition by stabilizers *Biophys. J.* **65** 661–71
- Ramesh J, Salman A, Hammody Z, Cohen B, Gopas J, Grossman N and Mordechai S 2001 FTIR microscopic studies on normal and H-ras oncogene transfected cultured mouse fibroblasts *Eur. Biophys. J.* **30** 250–5
- Small E W and Peticolas W L 1971 Conformational dependence of the Raman intensities from polynucleotides *Biopolymers* **10** 69–88
- Sophianopoulos A J, Rhodes C K, Holcomb D N and van Holds K E 1962 Physical studies of lysozyme *J. Biol. Chem.* **237** 1107–12
- Spiro T G and Garber B P 1977 Laser Raman scattering as a probe of protein structure *Annu. Rev. Biochem.* **46** 553–72
- Tennant T R, Kim H, Sokoloff M and Rinker-Schaeffer C W 2000 The Dunning model *Prostate* **43** 295–302
- van de Weert M, Haris P I, Hennick W E and Crommelin D J A 2001 Fourier transform infrared spectrometric analysis of protein conformation: effect of sampling method and stress factors *Anal. Biochem.* **297** 160–9
- Williams R W and Dunker A K 1981 Determination of the secondary structure of proteins from the amide I band of the laser Raman spectrum *J. Mol. Biol.* **152** 783–813
- Wilson W R and Hics K O 1999 Measurement of extravascular drug diffusion in multicellular layers *Br. J. Cancer* **79** 1623–6
- Yu N T, Jo B H and Liu C S 1972 A laser Raman spectroscopic study of the effect of solvation on the conformation of ribonuclease A *J. Am. Chem. Soc.* **94** 7572